JOURNAL OF SCIENCE TECHNOLOGY AND EDUCATION 10(3), SEPTEMBER, 2022
ISSN: 2277-0011; Journal homepage: www.atbuftejoste.com

An Optimized Sliding Mode Controller for Gantry Crane System Based on Smell Agent Optimization Algorithm

[1]Buhari, M. M., [2]Thuku, I. T., [3]Peter, Z. H., [4]Sani, S. K.
[1]*Department of Electrical and Electronics Technology, Federal Polytechnic Bali, Taraba state.*
[2]*Department of Electrical and Electronics Engineering, Modibbo Adams University Yola, Adamawa state,*
[3]*Department of Computer Engineering, Ahmadu Bello University Zaria, Kaduna state,*
[4]*Department of Computer Engineering, Kaduna Polytechnic, Kaduna state,*

ABSTRACT
Crane systems are a crucial part of the industrial machinery system used to transport heavy cargo or loads from one point to another. Technological advancement and operation environment requiring robust and high-speed operating cranes performing accurate position tracking irrespective of unwanted motion or disturbance is most required. However, this unwanted motion and disturbance is a crucial problem and a major setback in the control study of crane systems. Existing nonlinear controllers show a good system performance when compared to linear controllers whose performance deteriorates with an increase in operating range and uncertainty, hence, the need for a nonlinear controller that will guarantee system performance in presence of uncertainty. This study implements a sliding mode controller (SMC) augmented with Smell Agent Optimization (SAO) Scheme for stabilization and tracking of position coordinates in a gantry crane system (GCS). Modelling and simulation of the GCS with the developed controller were carried out using MATLAB/Simulink R2019b. Performance of the GCS with the developed controller was evaluated based on steady-state error, overshoot, and settling time as performance metrics and results compared with the SMC controller reported in the literature. Results analysis illustrate that the SMC-SAO outperformed the standard SMC controller in terms of system stabilization and set point tracking. SMC-SAO achieved a 46.12% and 83.50% reduction in settling time in terms of cart position and swing angle respectively. Also, SMC-SAO achieved a 99.99% reduction in steady-state error to swing angle.

ARTICLE INFO
Article History
Received: June, 2022
Received in revised form: June, 2022
Accepted: July, 2022
Published online: September, 2022

KEYWORDS
Gantry crane, Sliding Mode Controller, Smell Agent Optimization, Matlab.

INTRODUCTION

The use of cranes leads to a reduction in manual labour application, improved efficiency, and generally improved productivity of a system (Kang et al., 2017). These systems are crucial in transporting and lifting large and heavy material, containers, or blocks in construction sites, manufacturing, and transportation industries, and laboratory from one point within or around the desired destination (Abdullahi et al., 2018; Naskar & Pal, 2017). The crane consists of a hoisting mechanism, and support mechanism which is all mounted on the frame of the crane. The hoisting mechanism is commonly made up of a hoisting line and a hook that is suspended on the support mechanism which is made up of a trolley moving on a rail or girder (Abdel-Rahman et al., 2003). Based on the degree of freedom offered by the support mechanism to the suspension mechanism, three types of crane can be classified; boom, rotary, and gantry crane.

The boom cranes are usually mounted on mobile structures such as trucks, and ships for cargo transport of offshore constructions, and the rotary crane is preferred in the construction industries (Abdel-Rahman et

Corresponding author: Buhari, M. M. ✉ buharimuhammad722@gmail.com ✉ *Department of Electrical and Electronics Technology, Federal Polytechnic Bali.*

al., 2003). The gantry crane also known as the overhead crane support mechanism is made up of a rail or girder on which the trolley moves on, in other gantry cranes the girder is mounted on another rail that is horizontally placed on the previous rail.

(a) Boom Crane (b) Rotary Crane (c) Gantry Crane

In Figure 1. (a) is the pictorial representation of a boom crane; (b) is that of a rotary crane, and (c) is for a gantry crane. However, in the process of transporting such loads, load swinging occurred as a result of acceleration or deceleration of the crane which tends to affect the positioning precision of the load (Abdullahi et al., 2018). Undesirable crane motions or disturbances such as load bouncing, twisting, and swinging coupled with external disturbances such as wind are common during load hoisting operations. These factors affect the performance and productivity of the system drastically. These unwanted motions that consequently affect the precise positioning of the payload could result in accidents and damages to buildings or facilities that are close to the crane could occur due to the swinging or pendulation of the payload (Yoon et al., 2014), in a cluttered workspace like nuclear reactor zone, almost zero pendulation or swing of the load is expected during travelling stage and at load destination. (Abdel-Rahman et al., 2003). Unwanted motions characterized as inertial forces due to the prescribed motion of the payload and the excitation of the base is pronounced, slow manoeuvring or stopping the crane operation motion at intervals to dampen out the motion was used, but such technique introduced time delay, reduced crane efficiency and increased operating cost hence, the need for automatic control (Abdel-Rahman et al., 2003). Several conceptual and constructive control methods had been applied in the stabilization and adaptive control of nonlinear systems such as the crane, and most of these methods rely on the application of energy (Lyapunov) function to the construction of the control law or in a close loop analysis of the system (Astolfi & Ortega, 2003). Several control techniques among which include the time-optimal classical control, hybrid fuzzy-PID, input shapers, and SMC had been proposed for crane stabilization. Nevertheless, the presence of external disturbances and uncertainty during crane operation limits the efficiency of the proposed approach.

The past few years have seen research intensify in the design and control of crane systems. In (Renuka and Mathew (2013); Naskar and Pal (2017); Liu et al, (2018)) PID and fuzzy-PID have been suggested as a control strategy for reducing payload swing, and achieving load positioning and disturbance rejection for different crane models. (Pauluk (2016)) implemented linear quadratic regulator to reduce load swing in overhead cranes, LQR achieve 25% and 35% reduction in load swing for X and Z directions to the optimal control techniques compared. In Nguyen et al. (2017), SMC based on radial basis function (RBF) is implemented, RBF compensated for uncertainty nonlinear functions, the result, when compared with other controllers, shows better performance in terms of parametric variation and robustness, also better swing reduction was observed.

The stabilization controller was designed based on the immersion and invariance design concept by Li et al. (2013), and the control objective is to have all the systems state-regulated to zero. A nonlinear controller based on the Lyapunov function and Lassalle theorem was carried by Lu Biao et al. (2018), to design a control law for stability at the equilibrium point, the control technique was

Corresponding author: Buhari, M. M. ✉ buharimuhammad722@gmail.com ✉ *Department of Electrical and Electronics Technology, Federal Polytechnic Bali.*

compared with LQR, PID, and independent control methods, and the technique performs better in terms of swing reduction and position tracking. Abdullahi et al. (2018) implemented an adaptive output-based command shaping control technique for swing reduction in overhead crane systems, and simulation results compared with that of existing controllers (i.e. extra insensitive (EI) and zero-vibration-derivative-derivative control (ZVDD)) outperformed the other two input shaper controllers in terms of disturbance rejection and load swing reduction.

Chwa (2017) a non-linear anti-swing SMC controller is proposed for 3D crane model for reduced payload swing and desired position tracking of load. Sliding mode controller was implemented by Hussein et al., (2020) for lifting and conveying weighty load in overhead crane systems, asymptotic stability was carried using lyapunov functions, LQR controller is compared with the implemented SMC controller, both controller gave a satisfactory performance but SMC perform better. Despite the performance of the controller studied, oscillation at the output of the system was observed and it is valid for small operation range, also, performance specification of the crane control system is only met by most of the linear and nonlinear controllers for small parameter variation and narrow operating condition. Hence, the need to optimize the controller gains to improve on the controller to guarantee stability even with wide operation time. The aim of this work is to design a robust controller that will employed the use of smell agent optimization algorithm to optimize the gain parameters of SMC that can handle uncertainty and external disturbances during crane operation.

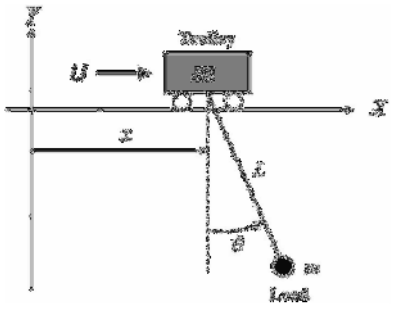

Figure 2: Model of a Gantry Crane Set-up (Naskar and Pal, 2017)

MATERIALS AND METHODS

In this section, the materials used and a detailed description of the methods followed to develop a sliding mode controller augmented with the SAO Scheme for stabilization and tracking of load position coordinates in the gantry crane system (GCS).

Materials

The materials used for the implementation of this work are presented. A 64-bit Windows 10 operating system HP desktop running on a 6.0GB RAM and an Intel Core i3 processor with MATLAB 2019b installed on it. There are several versions of Matrix Laboratory (MATLAB) that are available for use by the public. For this research, MATLAB/Simulink R2019b version available for use in the Electronics laboratory, department of Electrical engineering, Federal Polytechnic Beli, Taraba-Nigeria was used to carry out all simulation work,

Method

Modelling of Gantry Crane System

Mathematical modelling of the dynamics of the crane mostly used the Lagrange equation, Newton's second law of motion or Udwadia, and Kalaba motion equation (Kang et al, 2017), using physical laws and theories relating to the motion of the various parts that make up the system.

A typical setup of a gantry crane shows the moving cart (trolley) on a rail (girder), suspension cable, payload (load being transported), and the applied signal or input to the trolley. The crane with most acceptance in the transport, mining, and assembling lines is the gantry crane while for construction industries, rotary cranes are mostly employed (Abdel-Rahman et al., 2003b)

Corresponding author: Buhari, M. M. ✉ buharimuhammad722@gmail.com ✉ *Department of Electrical and Electronics Technology, Federal Polytechnic Bali.*

The set-up of a gantry crane is shown in Figure 2. where x is the displacement of the trolley, θ the angular displacement of the payload from the vertical position, u the control input, l the length of the hoisting cable, m and is mass of the payload, M is mass of the trolley and g is the acceleration due to gravity acting on the payload. The modelling of the crane system has two widely used approaches namely: Distributed-mass and lumped-mass models (Abdel-Rahman et al, 2003).In the distributed mass model, the payload and hook are lumped as a point mass, while the hoisting line is modelled as a distributed-mass, and are all used as a boundary condition to the distributed-mass system (Abdel-Rahman *et al*, 2003).

The distributed-mass model can be found in the work of (D'Andréa-Novel *et al*, 1992; d'Andréa-Novel *et al*, 1994) and that of (d'Andrea-Novel *et al*, 1991). This model neglects payload inertia and hoisting cable as inextensible and perfectly flexible material using the wave equation. In the lumped-mass model, the payload and the hook are lumped together and modelled as point mass while the hoisting cable is considered a massless cable (Abdel-Rahman *et al*., 2003). The entire structure of cable-hook-payload is considered to be a spherical pendulum. This model captured the complex dynamics of the payload motion and with this simple and compact model mathematical model can be formulated (Abdel-Rahman *et al*,2003; Renuka, 2013). The lumped-mass model is classified into two classes namely; the Reduced and Extended models based on the way the external inputs come into the system(Abdel-Rahman *et al*, 2003).

In general, special cases of the same classical models of the spherical pendulum that are influenced by base excitations are used to form reduced models of the crane (Abdel-Rahman *et al*, 2003). For this research work, a mathematical model of the gantry crane given in equation (1) and equation (2) from the work of (Hussein *et al*., 2020) will be adopted.

$$(M+m)\frac{d^2x}{dt^2}+mLcos\theta\frac{d^2\theta}{dt^2}-mLsin\theta\left(\frac{d\theta}{dt}\right)^2=u \quad (1)$$

$$mLcos\theta\frac{d^2x}{dt^2}-mL^2\frac{d^2\theta}{dt^2}+mgLsin\theta=0 \quad (2)$$

Where; M is the mass of the cart in (Kg), m represent the mass of the payload, L is the length of the hoisting (suspension) cable, g is the acceleration due to gravity, *u* is the applied control force or torque, x is the displacement of the trolley or distance travelled by the trolley and θ is the swing angle of the payload. Consequently, the dynamic model can transform form as follows;

$$\begin{bmatrix} M+m & mLcos\theta \\ mLcos\theta & mL^2 \end{bmatrix}\begin{bmatrix} \ddot{x} \\ \ddot{\theta} \end{bmatrix}=\begin{bmatrix} mL\dot{\theta}^2 sin\theta \\ -mgLsin\theta \end{bmatrix}+\begin{bmatrix} u \\ 0 \end{bmatrix} \quad (3)$$

Equation (4) can be expressed as follows:

$$\begin{bmatrix} K_{11} & K_{12} \\ K_{21} & K_{22} \end{bmatrix}\begin{bmatrix} \ddot{x} \\ \ddot{\theta} \end{bmatrix}=\begin{bmatrix} f_a+u \\ f_u \end{bmatrix} \quad (4)$$

Where;

$K_{11}=M+m, K_{12}=K_{21}=mLcos\theta$, $K_{22}=mL^2$, $f_u=-mgLsin\theta$, $f_a=mL\dot{\theta}^2 sin\theta$

Corresponding author: Buhari, M. M. buharimuhammad722@gmail.com *Department of Electrical and Electronics Technology, Federal Polytechnic Bali.*

Let us defined $K = \begin{bmatrix} K_{11} & K_{12} \\ K_{21} & K_{22} \end{bmatrix}$

Then equation (5) can be transformed into:

$$\begin{bmatrix} \ddot{x} \\ \ddot{\theta} \end{bmatrix} = K^{-1}(\theta)\begin{bmatrix} f_a + u \\ f_u \end{bmatrix} \quad (5)$$

Equation (11) can be transformed into the following equations (6) and (7) below

$$\ddot{x} = \frac{K_{22}f_a - K_{21}f_u}{K_{11}K_{22} - K_{12}K_{21}} + \frac{K_{22}f_a - K_{21}f_u}{K_{11}K_{22}} \quad (6)$$

$$\ddot{\theta} = \frac{-K_{11}f_a + K_{11}f_u}{K_{11}K_{22} - K_{12}K_{21}} + \frac{-K_{12}}{K_{11}K_{22}}u \quad (7)$$

Equation (6) and (7) can be written in a state space form as follows:

$$\ddot{x} = f_{11} + b_{11}u \quad (8)$$

$$\ddot{\theta} = f_{12} + b_{12}u \quad (9)$$

Where

$$f_{11} = \frac{K_{22}f_a - K_{21}f_u}{K_{11}K_{22} - K_{12}K_{21}}, \quad b_{11} = \frac{K_{22}}{K_{11}K_{22} - K_{12}K_{21}}$$

$$K_{22} = \frac{-K_{11}f_a + K_{11}f_u}{K_{11}K_{22} - K_{12}K_{21}}, \quad b_{22} = \frac{-K_{12}}{K_{11}K_{22} - K_{12}K_{21}}$$

The mathematical model presented in equations (1) to (9) defined above was modelled in Simulink to obtain the GCS model (X1, X2, X3, and X4). This model uses the front wheels for steering control and the back wheels for speed control. The Simulink model is given in figure 3.

Corresponding author: Buhari, M. M. ✉ buharimuhammad722@gmail.com ✉ *Department of Electrical and Electronics Technology, Federal Polytechnic Bali.*

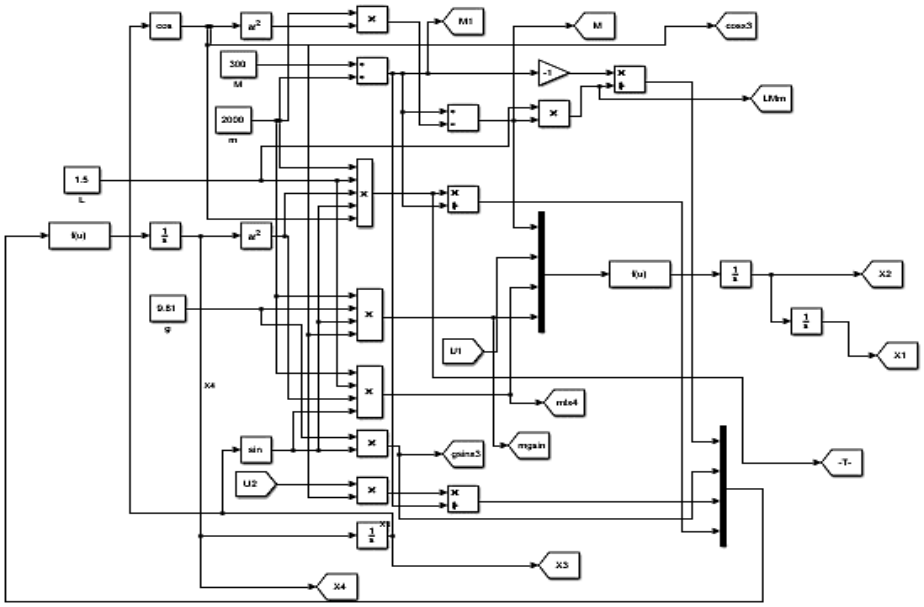

Figure 3: Developed Nonlinear Simulink Model of GCS

The Simulink model of the nonlinear GCS in Figure 3 is made up of a subsystem block used in obtaining the trigonometry functions, input port, and several output ports that represent system outputs.

Sliding Mode Control Technique

In this section, the control scheme is developed. It consists of a dynamic control design. The methodology is based on sliding mode control (SMC). Firstly, the system is transformed into a special structure through input transformation, containing a nominal part plus some unknown term. The unknown term is computed adaptively. The control problem is to find the control signal such that all the states of the system converge to zero. Based on the Lyapunov function, we are going to derive the dynamic control law in a series of steps, as follows: (Hussein et al., 2020).

The sliding mode function can be defined as:

$$s = \dot{x} + c_1 x + c_2 \dot{\theta} + c_3 \theta \qquad (10)$$

Where c_1, c_2 and c_3 are the controller parameters and they can be expressed as follows

$$c_2 = L - \frac{g}{11} \qquad (11)$$

$$c_1 = -6 / g\left(c_2 - L\right) \qquad (12)$$

$$c_3 = L c_1 + 6\left(c_2 - L\right) \qquad (13)$$

By differentiating equation (10) while substituting equations (8) and (9)

$$\dot{s} = f_1 + c_2 f_2 + \left(b_{11} + c_2 b_{22}\right) u + c_1 \dot{x} + c_3 \theta \qquad (14)$$

Corresponding author: Buhari, M. M. ✉ buharimuhammad722@gmail.com ✉ *Department of Electrical and Electronics Technology, Federal Polytechnic Bali.*

The control law can be expressed as:

$$u = -\frac{1}{b_{11+c_2 b_{22}}}\left[f_1 + c_2 f_2 + c_1 \dot{x} + c_3 \dot{\theta} + \zeta sgn(s) \right] \quad (15)$$

As seen in equation 15, the controller gains parameters are C_1, C_2 andC_3. The gains parameters have a direct impact on the system control law (U). The great the values of C_1, C_2 and C_3, the faster the system approached the sliding surface. Hence, control law (U) depends on the values of the gains parameters,C_1, C_2 and C_3.

Therefore, there is a need to employ an optimization algorithm to search for the optimal value of C_1, C_2 andC_3.

The sliding mode controller (SMC) was developed to minimize the trajectory tracking error of the load swing angle generated by the GCS. The SMC was designed in Simulink using equations (10) to (15).

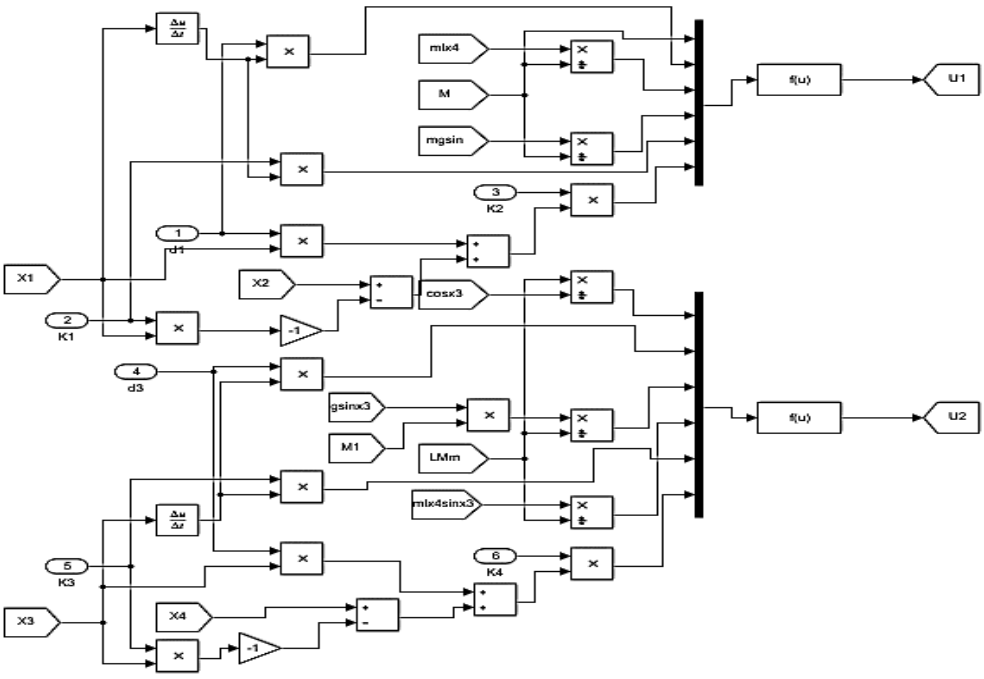

Figure 4: Simulink Model of SMC

Figure 4, is the Simulink model of the SMC controller containing five (5) controller parameters. To obtain the optimal values of the controller parameters, Smell Agent Optimization Algorithm (SAO) was designed to obtain the optimal parameters of the SMC controller (K1, K2, K3, K4, d1, d3). These parameters are the controller gains to be optimized to improve the performance of the SMC.

Smell Agent Optimization Technique

Smell agent optimization (SAO) is a class of optimization techniques inspired by the phenomenon of smell (Salawudeen et al., 2021). The optimization algorithm is based on the random concentration of smell particles and the detection capability of an agent. It considers the Brownian motion of the smell molecules and the movement of the agent towards this molecule. The SAO generates the initial population (position) of smell molecules and it then simulates the chemo-sensation process of the organism (agent). Each smell molecule represents a potential solution to the given problem. The SAO has three major modes which are; sniffing mode, trailing mode, and random mode (Salawudeen et al., 2021).

Corresponding author: Buhari, M. M. ✉ buharimuhammad722@gmail.com ✉ *Department of Electrical and Electronics Technology, Federal Polytechnic Bali.*

Sniffing Mode

This is the starting mode and the smell molecules evaporate from the smell source towards the agent. The agent evaluates the concentration of the smell molecule and follows the direction it's coming from. This process is initiated by generating a random initial position of smell molecules. The position of each smell molecule (potential solution) is determined by the position vector and molecules velocity and is given as (Salawudeen et al., 2021):

$$X_i^{(t+1)} = X_i^{(t)} + V_i^{(t+1)} \qquad (16)$$

Where $X_i^{(t+1)}$ is the updated molecule position, X_i^{t} is the previous molecule position, and $V_i^{(t+1)}$ is the updated velocity. The updated velocity $V_i^{(t+1)}$ is given as (Salawudeen et al., 2021):

$$V_i^{(t+1)} = V_i^{(t)} + r_0 \times \sqrt{\frac{3KT}{m}} \qquad (17)$$

Where V_i^{t} is current velocity, K is Boltzmann constant, T is the temperature of smell molecule, and m is the mass of the molecule. Therefore, equation (17) becomes:

$$X_i^{(t+1)} = X_i^{(t)} + \left(V_i^{(t)} + r_0 \times \sqrt{\frac{3KT}{m}} \right) \qquad (18)$$

Where r_0 is a random number that penalizes the third part of the equation. At the sniffing mode, the fitness of the updated position of the smell molecules is evaluated using equation (19). Hence, it is at this point that the agent X_{agent} sniffs the molecules with the best fitness and then updates its position based on the fittest.

Trailing Mode

After a decision has been made in the sniffing mode, the agent begins to follow the smell molecules to identify the source. The agent only trails the molecules with the highest concentration until the solution is found (smell source). This trailing behaviour of the agent is expressed as (Salawudeen et al., 2021).

$$X_i^{(t+1)} = X_i^{(t)} + r_1 \times olc \times \left(X_{agent}^{(t)} - X_i^{(t)} \right) - r_2 \times olc \times \left(X_{worst}^{(t)} - X_i^{(t)} \right) \qquad (19)$$

Where r_1 and r_2 are numbers generated randomly at various intervals. During trailing, r_1 and r_2 penalizes the influence of the olfaction capacity parameter on the agent's position and the worst position of the smell molecules respectively. By so doing, the movement of the agent is guided only within the position of the agent and that of the worst position of molecules.

Random Mode

In a situation where the agent loses its trail due to the discrete nature of the molecules, this situation may lead to entrapment of the agent in local minima and which leads to the inability to continue trailing. In such scenarios, the agent goes into the random mode. In this mode, the agent takes a step movement randomly in the search space and it is expressed as (Salawudeen *et al*., 2021)

$$X_i^{(t+1)} = X_i^{(t)} + r_3 \times SM \qquad (20)$$

Corresponding author: Buhari, M. M. ✉ buharimuhammad722@gmail.com ✉ *Department of Electrical and Electronics Technology, Federal Polytechnic Bali.*

Where SM is a constant indicating a step movement and r_3 is a random number which penalizes the value of the step movement.

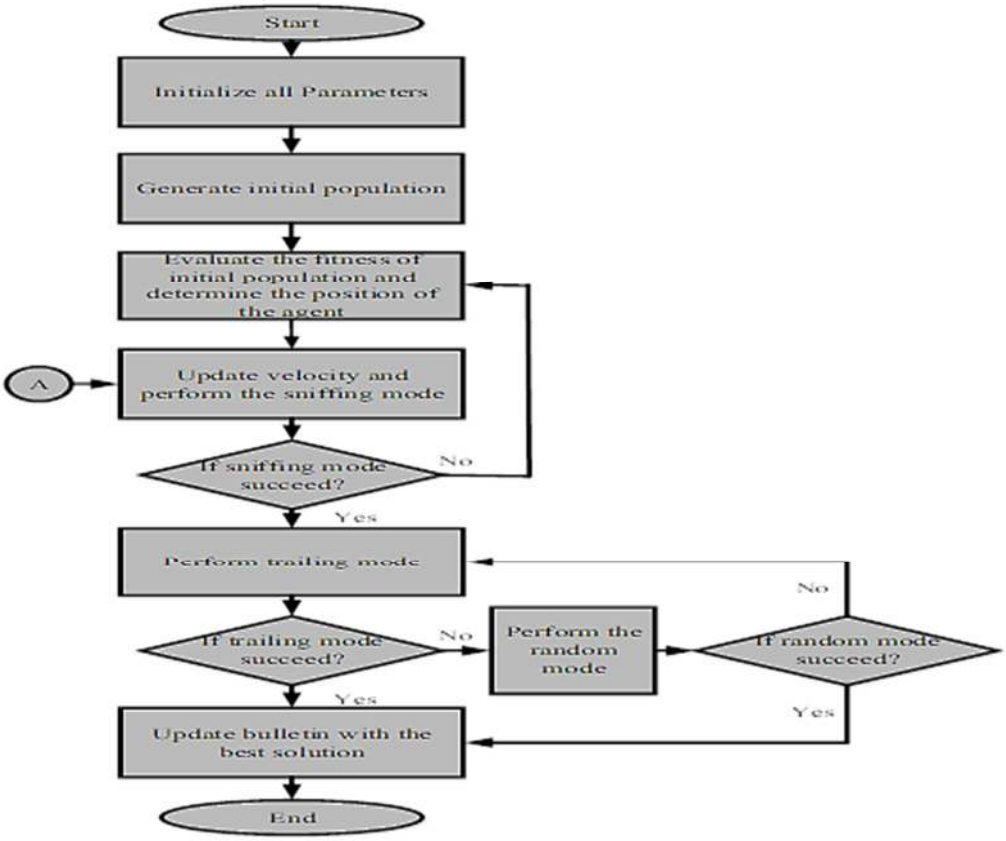

The flowchart of the smell agent optimization is shown (Salawudeen *et al*., 2021)

Figure 5: Flow Chart of SAO

Problem Formulation

The controller parameters to be optimized are (K1, K2, K3, K4, d1, d3) of the SMC obtained from the Simulink model of the SMC. These parameters are the controller gains to be optimized to improve the performance of the SMC. To obtain an optimized weight for the controller input, the weighting factor given in equation (21) was formulated into an objective function. The objective of the optimization problem is to minimize the weight by optimizing the weighting factor. The objective function is given as

$$F = \sqrt{\frac{\left(u_1 - u_{ref}\right)^2}{\sum u_1}} + \sqrt{\frac{\left(u_2 - u_{ref}\right)^2}{\sum u_2}} \qquad (21)$$

The optimum solution is determined subject to the constraints:

$$4 < d_1 < 6 \qquad (22)$$

Corresponding author: Buhari, M. M. ✉ buharimuhammad722@gmail.com ✉ *Department of Electrical and Electronics Technology, Federal Polytechnic Bali.*

$$1<k_1<2 \quad (23)$$

$$1 < k_2 < 2 \quad (24)$$

$$4 < d_3 < 6 \quad (25)$$

$$1.5 < k_3 < 2 \quad (26)$$

$$1 < k_4 < 2 \quad (27)$$

Therefore K1, K2, K3, K4, d1, and d3 are the parameters of the weighting factor that must be optimized to achieve the objective function.

Optimization of the Weighting Factor using SAO

The cost function parameter is optimized using the SAO algorithm. Equation (21) serves as evaluation criteria. In the beginning stage, the initial population of size N is generated, and the values of the weighting factor parameters are randomly selected based on the constraints given in equations (22) to (27). Then the selection process of the SAO is carried out in such a way that it searches for the best combination of the parameters that will obtain the optimal solution. In search of the optimum of the objective function, the three modes of the algorithm (sniffing, trailing, and random mode) are used. The parameters in the search space follow the trail of the best small molecule. The weighting factor cost function is optimized until the termination criteria are reached. The SAO parameters used in this research are given in Table 1.

Table 1: SAO Parameters

S/N	Parameter	Symbol	Value	Unit
1	Mass	M	2.4	Kg
2	Temperature	T	3	K
3	Boltzmann's Constant	K	1.38×10^{-23}	JK^{-1}
4	Population (Molecules)	N	50	-----
5	Dimension	D	3	-----
6	Iteration	Itr	30	------
7	Step Movement	SM	2.5	M

Corresponding author: Buhari, M. M. ✉ buharimuhammad722@gmail.com ✉ *Department of Electrical and Electronics Technology, Federal Polytechnic Bali.*

The simulation of the developed SMC-SAO with the GCS given in Figure 8 was simulated under different initial conditions (IC) using the close loop system developed in Simulink/MATLAB as shown in Figure 8.

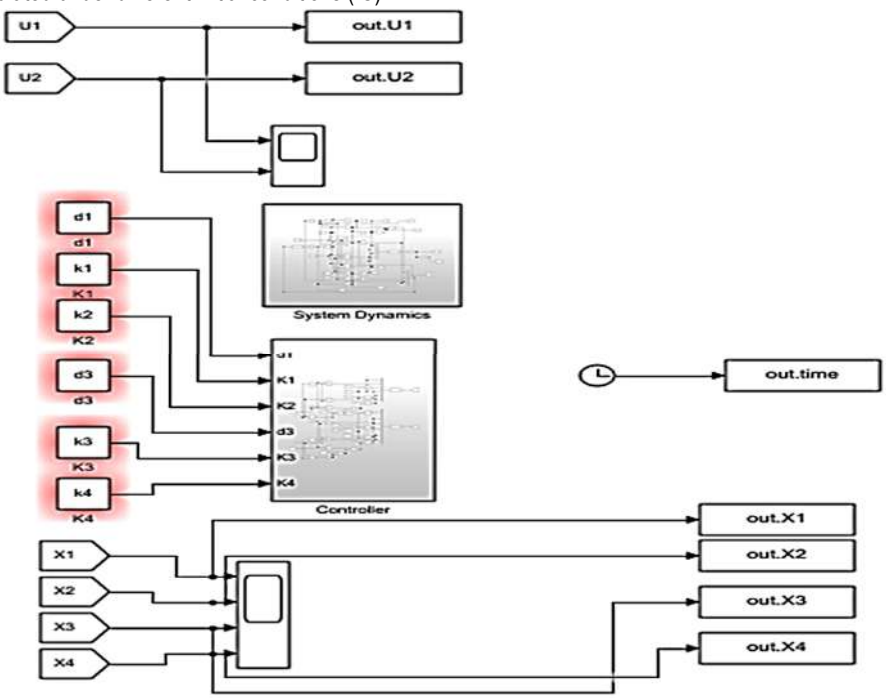

Figure 8: Simulink Model of GCS using Optimized SMC

The Simulink model developed for control of the GCS using SMC-SAO is made of a subsystem block that represents the dynamics of GCS and the controller, a gain the parameters of the controller to be optimized. The scopes displayed the response of the states of the system and that of the control law.

Performance Evaluation

Performance metrics are metrics used to determine the performance improvement, effectiveness, efficiency, and appropriate levels of internal controls of a system (Alagoz et al., 2015). Amongst the performance, metrics to be considered in this work are the transient response and the steady-state response. The transient response is the response of the system that goes from the initial state to the final state until the system becomes stable. The main parameters of the transient response of the system are: settling time, and overshoot (Ogata, 2010), while the steady-state is one of the parameters used for measuring the relative stability of the system. It is the response of the system after it has finally settled.

Settling Time

This is one of the time specifications of the transient state. It is the time required for the response to reach the steady state and stay within a specified tolerance band around the final value. In general, the tolerance band is between 2% to 5%.

Overshoot

This is also one of the time specifications in a control system. It is the deviation of the response at peak time from the final value response.

Steady-state Error

The transient response of a practical control system often exhibits damped oscillation before reaching a steady state. If the output of the system at the steady-state does not exactly agree with the input, such a system is said to have a steady-state error. It is the value of the error signal when time $t \rightarrow \infty$. The SSE is the measure of system accuracy (Alphinas *et al*.,2017).

Corresponding author: Buhari, M. M. buharimuhammad722@gmail.com *Department of Electrical and Electronics Technology, Federal Polytechnic Bali.*

The metrics mentioned above were used to evaluate performance improvement using the formula in Equation (34).

$$\eta = \frac{K_{SMC} - K_{SAO-SMC}}{K_{SMC}} \times 100\% \quad (28)$$

Where η represents the percentage improvement of the developed SAO-SMC over the sliding mode controller (SMC), K_{SMC} is the value obtained on the sliding mode controller and $K_{SAO-SMC}$ is the value obtained when SAO-SMC was used.

RESULT AND DISCUSSION

The simulation results obtained based on the methodologies that addressed the research objectives are discussed and compared with the work of (Hussein *et al*., 2020). The results obtained for both stabilization and set point tracking of the system states are presented in this section.

Convergence of Smell Agent Optimization

Smell Agent Optimization is used in optimizing the parameters of SMC, the convergence of the optimizer on the designed SMC-SAO controller is given in the simulation graph in figure 8.

Figure 8: SAO Convergence plot on Benchmark System

Figure 8. Shows the SAO convergence on the benchmark model, the algorithm converged at the 24th iteration with an optimized cost function. The SMC was tuned to search for best gains using SAO, after running 50 iterations, the best parameters were found as shown in table 2.

Table 2: Properties of Best Smell Object

SAO Parameters	Value
Cost Function	1.61473904073533e+06
d_1	4.877
K_1	1.4463
K_2	2.8329
d_3	4.4193
K_3	1.7402
K_4	1.113

Stabilization Results

The results of the stabilization of the system using the developed SAO sliding mode controller under different initial conditions (ICs) of [0.98 0.2 pi/16 pi/8], and [0.5 1.2 pi/8 pi/4] which represent the position of the system states were given in the results presented in the figures that follow. From the analysis of Figure (9), it can be seen that there was a shape rise in the amplitude of the trolley position of the GCS when an input signal was applied to the system when using SMC without SAO. However, when using the SAO-SMC was reduced and the controller was able to stabilize it faster to zero equilibrium point and the oscillation was less when compared to the existing scheme using SMC without SAO. It implies the controllability of the linear displacement state. This shows that the SAO-SMC provides improved dynamic stability for the GCS during operation.

Corresponding author: Buhari, M. M. ✉ buharimuhammad722@gmail.com ✉ *Department of Electrical and Electronics Technology, Federal Polytechnic Bali.*

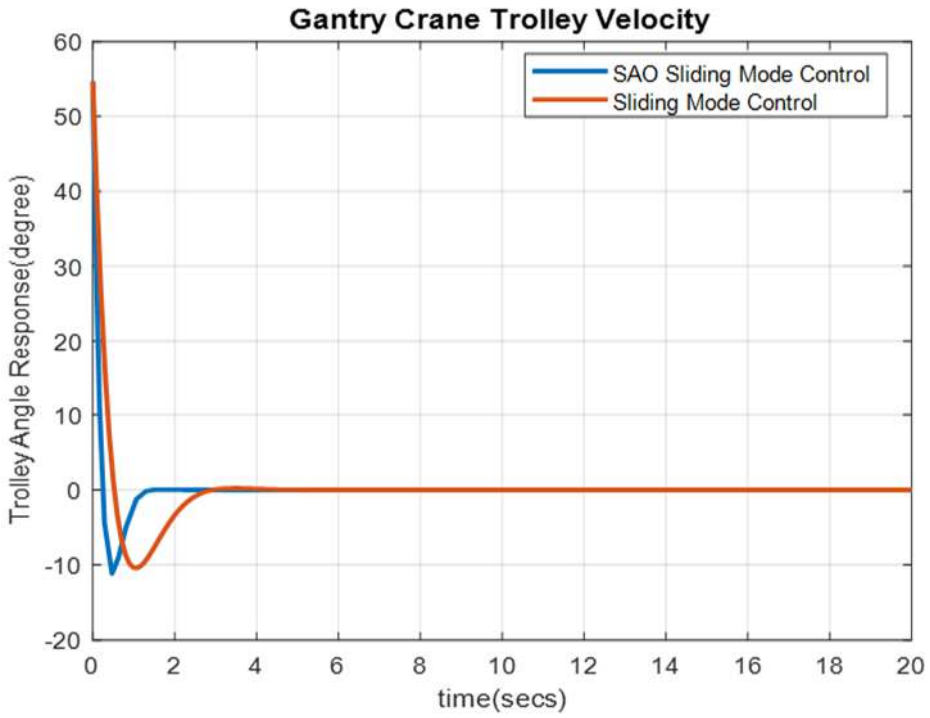

Figure 9: Linear displacement of the cart

Corresponding author: Buhari, M. M. ✉ *buharimuhammad722@gmail.com* ✉ *Department of Electrical and Electronics Technology, Federal Polytechnic Bali.*

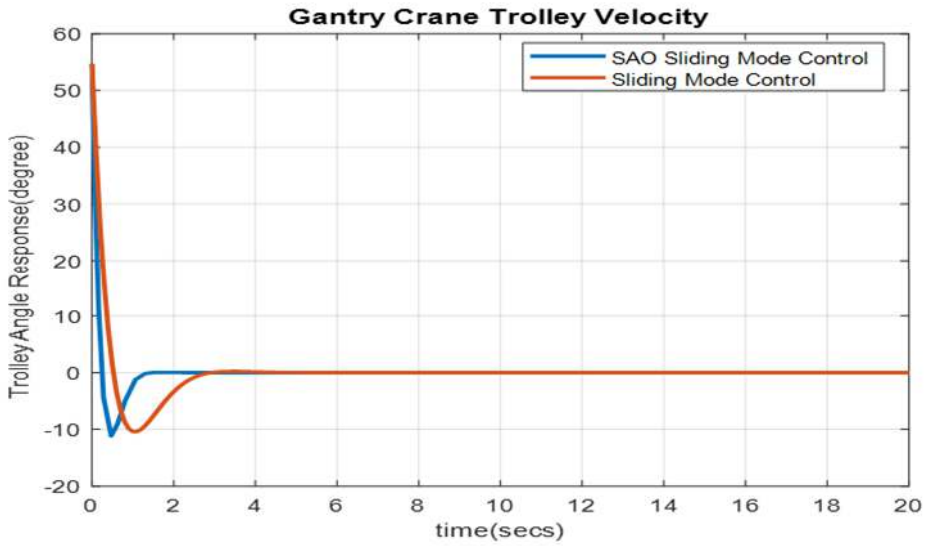

Figure 10: Linear speed of the cart

In Figure 10, it was observed that the linear speed of the cart using SMC without a controller was having a longer amplitude at the initial point, but later stabilized to zero equilibrium point when the controller acted based on the error signal generated. However, using SAO-SMC, the amplitude of the trolley settle faster to the equilibrium position showing improvement over SMC without SAO.

Figure 11, shows the load swing angle of the GCS. From the figure above, it was observed that using the SMC without SAO, the swing angle takes a longer time to stabilize to the equilibrium point. However, using SMC-SAO, the swing angle stabilize faster to the equilibrium point which implies the system states controllable.

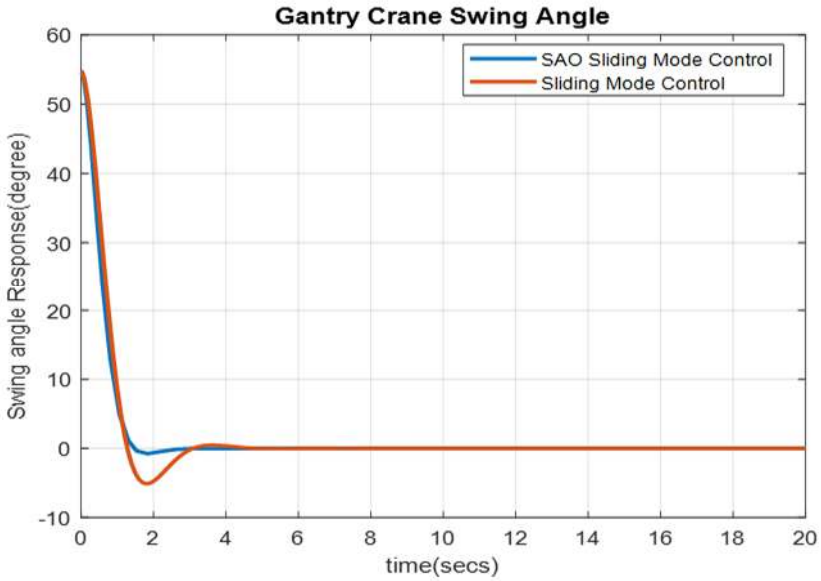

Figure 11: Load swing angle

Corresponding author: Buhari, M. M. ✉ *buharimuhammad722@gmail.com* ✉ *Department of Electrical and Electronics Technology, Federal Polytechnic Bali.*

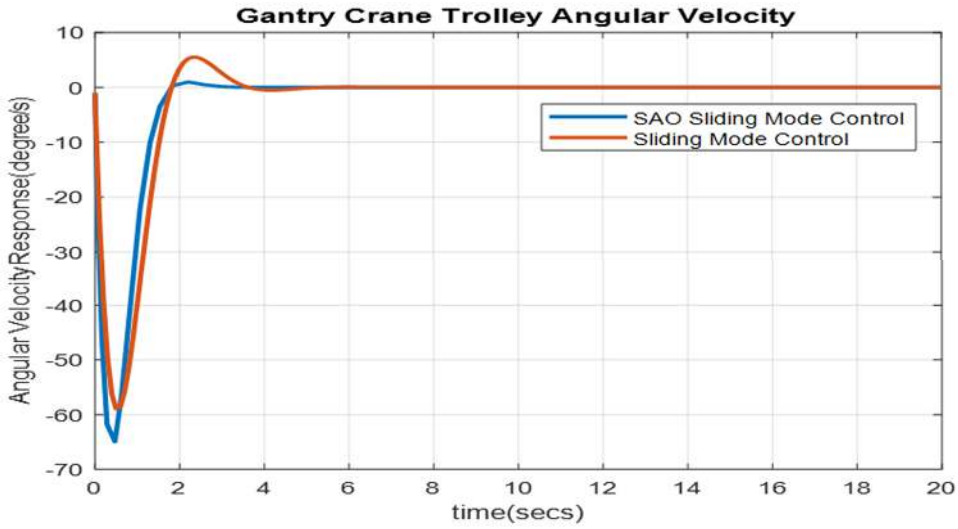

Figure 12: Load angular speed

Figure 12 shows the angular velocity of the GCS. From the figure above, it was observed that the angular velocity using the developed SAO-SMC, there is a rise in amplitude due to the transient nature of the system, but it later converges faster to the equilibrium. Using controller-based SMC without SAO, there is a sharp rise in amplitude, which occurred due to the transient nature of the system but it took a long time to stabilize and converged to the equilibrium. The controller responsible for system stabilization under the first given initial conditions is given in Figure 13.

Figure 13: Stabilizing Control action

Figure 13 shows control action u (t) that stabilized the states of the GCS under the given initial conditions stated early. It was observed that the amplitude of the control action of the SMC without SAO was large at some point due to the sharp rise in the system state compared to SAO-SMC. But later the SAO-SMC settles at zero before SMC without a controller when the states stabilized at the desired equilibrium. Control input of the SMC without SAO shows rapid changes which are dangerous in the case of practical application. Moreover, the developed controller with SAO requires less amount of control effort as compared to SMC without SAO.

Performance Comparison

The system performance with the developed controller was compared to the SMC reported in (Hussain *et al*., 2020) based on settling time, overshoot, and steady-state error, and the results were presented in Table 3.

Table 3: Performance Comparison between developed SAO-SMC and SMC

Performance Specification		Controller		Percentage Improvement (%)
		SMC-SAO	SMC	
Swing angle	Swing angle	Settling Time(s)	1.938	3.597
	Overshot (%)	0.417	2.527	83.50
	Steady-state error (m)	0.01	0.001	99.99

Table 3, summarizes the performance comparison of the developed SAO-SMC and SMC controller without SAO reported in (Hussein *et al*., 2020). It can be observed that the developed controller outperformed the SMC

Corresponding author: Buhari, M. M. ✉ buharimuhammad722@gmail.com ✉ *Department of Electrical and Electronics Technology, Federal Polytechnic Bali.*

without SAO in terms of settling time, overshoot, and steady-state error minimization

CONCLUSION

This research has presented the development of a sliding mode controller augmented with an SAO Scheme for stabilization and tracking of load position coordinates in the gantry crane system (GCS). The model of the GCS was developed in Simulink. Subsequently, an optimal control approach using SMC and SAO based on the formulated objective function was developed. The simulation was carried out in MATLAB/Simulink 2019b. The performance evaluation of the results was carried out and compared to the GCS developed by (Hussein *et al*., 2020) in terms of settling time, overshoot, and steady-state error.

The simulation results reveal the better performance of the developed controller when compared to the controller presented in (Hussein *et al*., 2020) with a 46.12% reduction in settling time in terms of load swing. While this work reports an 83.50% reduction in overshoot of load swing respectively. Additionally, it showed a 99.99% reduction in steady-state error for load swing. Hence, a solution to problems of load swing and precise load positioning in crane operation is presented. Even though SAO performs well in tracking problems, it has a problem of longer Convergence time. The convergence time can be improved by modifying the algorithm.

REFERENCES

Abdel-Rahman, E. M., Nayfeh, A. H., & Masoud, Z. N. J. M. A. (2003). Dynamics and control of cranes: A review. *Journal of Vibration and Control, 9*(7), 863-908. DOI: DOI: 10.1177/1077546303009007007

Abdullahi, A. M., Mohamed, Z., Selamat, H., Pota, H. R., Abidin, M. Z., Ismail, F., . . . Processing, S. (2018). Adaptive output-based command shaping for sway control of a 3D overhead crane with payload hoisting and wind disturbance. *98*, 157-172.

Alagoz, B. B., Deniz, F. N., Keles, C., and Tan, N. (2015) Disturbance rejection performance analyses of closed-loop control systems by reference to disturbance ratio. *ISA transactions, 55*, 63.

Alphinas, R. A., Hansen, H. H., and Tambo, T. (2017). Comparison of the conventional closed-loop controller with an adaptive controller for a disturbed thermodynamic system. Paper presented at the 2017 Evolving and Adaptive Intelligent Systems (EAIS).

Astolfi, A., & Ortega, R. J. I. T. o. A. c. (2003). Immersion and invariance: a new tool for stabilization and adaptive control of nonlinear systems. *48*(4), 590-606.

Chwa, D. J. I. T. o. I. E. (2017). Sliding-Mode-Control-Based Robust Finite-Time Antisway Tracking Control of 3-D Overhead Cranes. *64*(8), 6775-6784.

D'Andréa-Novel, B., Boustany, F., & Conrad, F. (1992). Control of an overhead crane: Stabilization of flexibilities *Boundary control and boundary variation* (pp. 1-26): Springer.

d'Andréa-Novel, B., Boustany, F., Conrad, F., Rao, B. J. M. o. C., Signals, & Systems. (1994). Feedback stabilization of a hybrid PDE-ODE system: Application to an overhead crane. *7*(1), 1-22.

d'Andrea-Novel, B., Boustany, F., & Rao, B. (1991). *Control of an overhead crane: Feedback stabilization of a hybrid PDE-ODE system.* Paper presented at the Proceedings of the 1st European Control Conference: ECC.

Emad. Q. Hussein, Ayad. Q Al-Dujaili & Ahmed, R., Ajel. (2020). *Design of sliding mode control for overhead crane systems: Theory and experimentation.* Paper presented at the 3rd International Conference on Sustainable Engineering Technique, Proceedings.

He, X., Shi, J., He, W., & Sun, C. J. I.-P. (2017). Boundary vibration control of a variable length crane system in two-dimensional space with output constraints. *50*(1), 11996-12001. .

Corresponding author: Buhari, M. M. ✉ buharimuhammad722@gmail.com ✉ *Department of Electrical and Electronics Technology, Federal Polytechnic Bali.*

Kang, H., Shunqiang, S., Shengchao, Z., Xinfang, G., & Yongqi, Z. J. P. o. t. I. o. M. E., Part E: Journal of Process Mechanical Engineering. (2017). Dynamic analysis and tracking trajectory control of a crane. *231*(5), 1045-1052.

Li, S., Liu, X., Dong, X., Jing, Y., Liu, X. J. I. J. o. I. C., Information, & Control. (2013). A novel controller for a class of nonlinear systems via immersion and invariance. *9*(8), 3463-3470.

Liu, X., Li, W., Wang, W., & Xu, Z. J. A. J. o. C. (2018). Control for the New Harsh sea Conditions Salvage Crane Based on Modified Fuzzy PID.

Lu Biao, Fang Yongchun, & Ning, S. (2018). Modelling and nonlinear coordination control for an underactuated dual overhead crane system. *Automatica, 91*, 244-255.

Naskar, I., & Pal, A. (2017). *Type-2 Fuzzy Controller with Type-1 Tuning Scheme for Overhead Crane Control.* Paper presented at the International Conference on Computational Intelligence, Communications, and Business Analytics.

Nguyen, N. P., Ngo, Q. H., & Nguyen, C. N. (2017). *Adaptive sliding mode control using radial basis function network for container cranes.* Paper presented at the Control, Automation and Systems (ICCAS), 2017 17th International Conference on.

Ogata, K., & Yang, Y. (2002). *Modern control engineering* (Vol. 4): Prentice hall India.

Pauluk, M. J. P. E. (2016). Optimal and robust control of the 3D crane. *92*(2), 206--212.

Renuka, V., & Mathew, A. T. J. I. J. T. A. R. M. E. (2013). Precise Modelling of a Gantry Crane System Including Friction 3D Angular Swing and Hoisting Cable Flexibility. *2*, 119-125.

Salawudeen, A. T., Mu'azu, M. B., Yusuf, A., & Adedokun, A. E. (2021). A Novel Smell Agent Optimization (SAO): An extensive CEC study and engineering application. *Knowledge-Based Systems*, *232*, 107486.

Yoon, J., Nation, S., Singhose, W., & Vaughan, J. E. J. I. T. o. C. S. T. (2014). Control of crane payloads that bounce during hoisting. *22*(3), 1233-1238.

Corresponding author: Buhari, M. M. ✉ *buharimuhammad722@gmail.com* ✉ *Department of Electrical and Electronics Technology, Federal Polytechnic Bali.*